Journal Pre-proof

Major body size change in an extinct tropical island mammal associated with glacial-interglacial environmental shifts

Samuel T. Turvey, Angela L. Lamb, Phil Rye, Abel Vale Nieves, Joanne H. Cooper, Peter van Calsteren

PII: S2589-0042(25)02229-1

DOI: https://doi.org/10.1016/j.isci.2025.113968

Reference: ISCI 113968

To appear in: *iScience*

Received Date: 16 June 2025

Revised Date: 27 August 2025

Accepted Date: 2 October 2025

Please cite this article as: Turvey, S.T., Lamb, A.L., Rye, P., Nieves, A.V., Cooper, J.H., van Calsteren, P., Major body size change in an extinct tropical island mammal associated with glacial-interglacial environmental shifts *iScience* (2025), doi: https://doi.org/10.1016/j.isci.2025.113968.

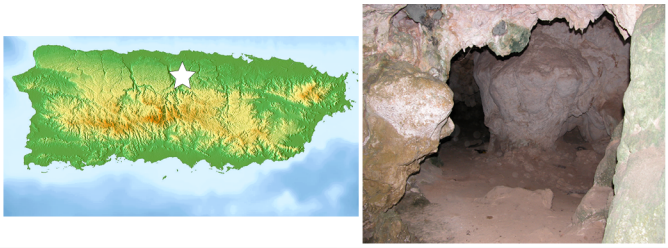

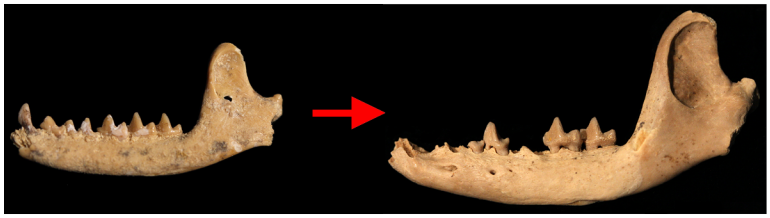

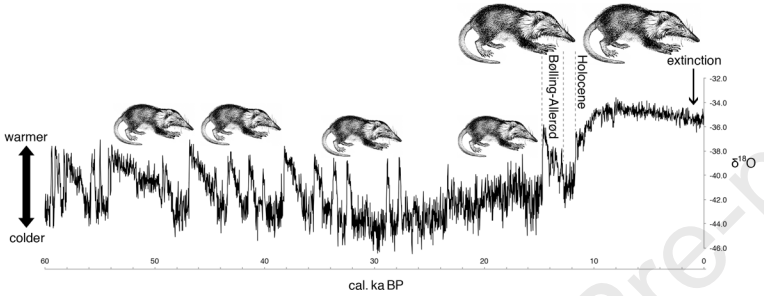

Major body size change in an extinct tropical island mammal associated with glacial-interglacial environmental shifts

Samuel T. Turvey[1,6,*], Angela L. Lamb[2], Phil Rye[3], Abel Vale Nieves[4], Joanne H. Cooper[3], Peter van Calsteren[5]

[1]*Institute of Zoology, Zoological Society of London, Regent's Park, London NW1 4RY, UK*

[2]*National Environmental Isotope Facility, British Geological Survey, Keyworth, Nottingham NG12 5GG, UK*

[3]*Bird Group, Department of Zoology, The Natural History Museum, Akeman Street, Tring, Hertfordshire HP23 6AP, UK*

[4]*Ciudadanos del Karso, 267 Sierra Morena PMB 230, San Juan 00926, Puerto Rico*

[5]*Department of Environment, Earth & Ecosystems, The Open University, MK7 6AA, UK*

[6]Lead contact

*Corresponding author: samuel.turvey@ioz.ac.uk

Summary. Patterns of late Quaternary body size change in small-bodied vertebrates remain poorly understood. The now-extinct Puerto Rican island-shrew *Nesophontes edithae* exhibits size variation across late Quaternary sites, but the chronology and correlates of this variation are unclear. Nesophontid material from two Pleistocene-Holocene sites demonstrates that a small morph was present for >30,000 years during the Last Glacial Period and was replaced by a large morph after the Last Glacial Maximum. Differing $\delta^{13}C$ values indicate the small morph was associated with open savanna and the large morph was associated with tropical forest. This allochronic change does not match the Island Rule or Bergmann's Rule, and may have been driven by an end-Pleistocene shift to high-productivity forest. Size morph replacement could reflect distributional shifts in niche-differentiated species or a rapid evolutionary response to climatic change. Our study demonstrates the resilience of some species to natural change but their vulnerability to anthropogenic pressures.

Keywords: climatic change, island evolution, late Quaternary, microevolution, *Nesophontes*, punctuated equilibrium, size differentiation

INTRODUCTION

Late Quaternary climatically-driven environmental changes had substantial impacts on terrestrial vertebrate communities. As well as being implicated in the global extinction of approximately 100 megafaunal mammal genera[1-3], climatic and vegetational shifts across the Pleistocene-Holocene boundary are also associated with allochronic body size reductions in many large-bodied vertebrate lineages[1,4-6]. Patterns of Quaternary body size change in large-bodied mammals are often used as support for the 'Island Rule', an extensively debated theme in island biogeography proposes that large species typically become smaller on islands, whereas small species become larger[7-9]. This phenomenon is shown most clearly by dwarfed populations of large-bodied mammal taxa (e.g. proboscideans, cervids, xenarthrans) that became isolated on small islands by rising sea-levels during the late Quaternary, and experienced evolutionarily rapid decreases in body size associated with reduced resource availability[10-12]. Other megafaunal taxa representing ancient insular lineages also show considerable fluctuations in body size over short timescales during the late Quaternary in response to rapid sea-level changes[13].

Conversely, less is known about patterns of faunal turnover or morphological change in small mammals over the late Quaternary. Many small-bodied lineages are known to have increased considerably in body size following isolation on islands, consistent with the Island Rule, but these changes typically occurred over longer evolutionary time-periods[7-9,14]. Some small mammal populations are also known to have experienced size decreases across the late Quaternary[15,16], and decreases in body size that contradict expectations of the Island Rule and may instead be associated with late Quaternary temperature

change ('Bergmann's Rule') are documented in some insular rodents and eulipotyphlan insectivores across the Pleistocene-Holocene boundary[17,18]. Allochronic size variation in small-bodied island mammals across periods of late Quaternary climatic change may therefore be influenced by a range of environmental selection pressures, and the wider patterns, rates, and ecological correlates of morphological change in such taxa remain poorly understood.

The insular Caribbean contained one of the world's most diverse non-volant island mammal faunas for much of the late Quaternary, although nearly all of these species became extinct during the Holocene, probably due to human activities[19]. One of the most unusual components of the Caribbean land mammal fauna was the now-extinct nesophontids or 'island-shrews' (*Nesophontes* spp.), small-bodied eulipotyphlan insectivores with an ancient evolutionary history[20]. Nesophontid individuals from Holocene contexts in Cuba and Hispaniola show substantial size variation, which radiometric, morphometric and phylogenetic analyses have shown to represent multiple co-occurring size-differentiated species[21-23]. Considerable size variation is also observed in late Quaternary nesophontid samples from Puerto Rico, where island-shrews persisted into the late Holocene[24]. Only one species, *Nesophontes edithae*, has been described from Puerto Rico[25]; it is the largest known island-shrew, possibly due to ecological release in the absence of co-occurring large-bodied solenodons on this island. Puerto Rican nesophontids differ morphologically from all other Caribbean nesophontids (e.g., larger size, relative lack of reduction of third premolars compared to second premolars, larger relative size of third lower molar compared to second lower molar[26]), indicating that the presence of different morphs does not represent overwater colonization by a known species from

86 another island, and estimated evolutionary divergence times between other
87 nesophontid species substantially pre-date the known or inferred age of late
88 Quaternary Caribbean fossil sites containing nesophontid material[22]. Size
89 variation in late Quaternary samples from the island has instead been variously
90 interpreted as sexual dimorphism, multiple co-occurring endemic species, or
91 allochronic plasticity[21,25,27,28]. Indeed, as large-scale sexual dimorphism is
92 unknown in other recent eulipotyphlans, this variation was used as part of the
93 justification for erecting a new family, Nesophontidae, to accommodate the
94 genus[25].

95 Puerto Rico experienced a substantial decrease in subaerial land area across
96 the Pleistocene-Holocene boundary, with predominant Caribbean vegetation
97 types shifting from open savannah to closed moist broadleaf tropical forest
98 during this period[29-31]. These shifts constitute major environmental drivers of
99 biodiversity change, and could have been associated with phenetic change in the
100 island's terrestrial fauna. However, well-stratified Quaternary palaeontological
101 deposits are rare in Caribbean caves, and early collectors often failed to record
102 the stratigraphic provenance of Caribbean Quaternary material, resulting in
103 mixing of potentially allochronic nesophontid material within cave sites.
104 Although stable isotope analysis has been used to reconstruct the trophic
105 ecology of some extinct Caribbean species[32-34], diagenetic loss of collagen and
106 other complex biomolecules through geologically recent sample degradation
107 under tropical conditions is also a persistent problem for Caribbean Quaternary
108 fossils, limiting the potential for radiometric dating and phylogenetic analysis for
109 many specimens[19]. A dated temporal-ecological framework for interpreting size
110 variation in *N. edithae* against regional late Quaternary climatic and

111 environmental changes, to identify correlates of body size evolution in small-
112 bodied island mammals, has therefore remained elusive.
113 During palaeontological excavations in the northern karst belt of Morovis
114 Principality, Puerto Rico in 2005, we collected new nesophontid material from
115 two adjacent late Quaternary fossil sites: Nesophontes Cave, a previously
116 excavated site[35], and Nesophontes II Cave, which was discovered during our
117 fieldwork. This material demonstrates substantial morphological size variation,
118 and we are able to demonstrate that Puerto Rican nesophontids of differing sizes
119 are associated with different temporal horizons and past environmental
120 conditions, providing an important example of plasticity in phenotypic response
121 to Quaternary environmental change by a small-bodied island mammal.
122
123 **RESULTS**
124
125 **Fossil sites**
126 Nesophontes II Cave (2030320 N, 0769577 E) consists of a short (<10m) raised,
127 closed passageway immediately adjacent to the southern entrance of
128 Nesophontes Cave. The new site contained a rich deposit of small-bodied
129 vertebrate bones below a ledge against the eastern wall of the cave
130 approximately 8m from the entrance, consisting of >10,000 individual remains in
131 total. Based on faunal composition, highly localized accumulation, and pattern of
132 skeletal modification (e.g. skull, mandibular ascending ramus and long bone
133 breakage; surface corrosion from digestive acids[36]), this deposit is interpreted as
134 a prey accumulation made by an owl, probably the now-extinct endemic owl *Tyto*
135 *cavatica*[37]. The deposit extended from the sediment surface to a depth of 30cm

and contained an extremely dense lens of bones between 20–24cm depth (Fig. 1). The entire deposit was excavated and collected. Cranial and postcranial elements of *N*. *edithae* were abundantly represented throughout most of the deposit (although there were few well-preserved specimens from the oldest layers). The deposit also contained five bat species, a diverse bird assemblage containing at least 39 genera, large amounts of lizard material, and a second extinct endemic non-volant mammal (the caviomorph rodent *Heteropsomys insulans*) (Table S1). Bones collected from 0–24cm depth ('upper layer') were pale to dark brown in colour, whereas bones collected from below the dense lens (24-30cm, 'lower layer') were paler yellow in colour and often partially veneered by a thin calcite coating, suggesting two distinct depositional intervals.

Collection of further Quaternary mammal fossil material including *N*. *edithae* and other extinct endemic mammal taxa (the sloth *Acratocnus odontrigonus* and the giant caviomorph rodent *Elasmodontomys obliquus*) was also conducted through opportunistic sampling of the top 20 cm of unstratified paleosol deposits in the southern entrance slope of the neighbouring Nesophontes Cave (see ref. 35 for a description of this site). Fossil material from this site similar in preservational appearance to the deepest fossil material recovered from Nesophontes II Cave.

Morphometric comparisons

Nesophontes edithae specimens from the upper layer at Nesophontes II Cave are markedly larger and correspondingly more robust than specimens from the lower layer and from the entrance slope of Nesophontes Cave (Fig. 2). Unfortunately, damage to both cranial and postcranial elements characteristic of

owl predation[36] limits quantitative analysis of size differences using many standard mandibular or postcranial measurements, and nearly all specimens are too damaged to permit more complex multivariate morphometric analysis such as principal component analysis, which has been used to understand patterns of intraspecific and interspecific variation in nesophontids from other Caribbean islands[21,22]. It also precludes analysis of the small number of nesophontid specimens from the lower Nesophontes II layer (<25 fragmentary specimens in total, with 3-4 comparative measurements only possible for three femora). However, specimens from the upper layer are significantly larger than those from Nesophontes Cave in statistical comparisons of eight mandibular characters (comparative sample sizes: upper Nesophontes II layer, n=19-99; Nesophontes Cave, n=10-21) and eight femoral characters (comparative sample sizes: upper Nesophontes II layer, n=8-113; Nesophontes Cave, n=10-26) (one-tailed heteroscedastic t-tests, $p \leq 0.01$ for all statistical comparisons, $p \leq 0.0001$ for 14 of 16 comparisons; Table S2). The largest measurement datasets show different unimodal size distributions for specimens from the upper Nesophontes II layer and from Nesophontes Cave, indicating a single size morph is present in each deposit (Fig. S1).

Using established regression equations for calculating eulipotyphlan body masses from M1 and m1 length-width proportions[38], we estimate that individuals from the upper Nesophontes II layer had a mean body mass of 202.6g (n=31, SD=51.9), whereas individuals from the lower Nesophontes II layer had a mean body mass of 98.1g (n=7, SD=21.4), and individuals from Nesophontes Cave had a similar mean body mass of 82.9g (n=19, SD=13.2).

Temporal framework

Owl and other raptor-derived prey accumulations associated with suitable perches or roost/nest sites can be deposited by different individuals over thousands or tens of thousands of years[39,40]. A possible Late Pleistocene age for the lower Nesophontes II layer was suggested by the occurrence of the bat palaeosubspecies *Stenoderma rufum anthonyi*[27] in this level. Pre-screening of 40 fossil bone samples from the two caves (35 *N*. *edithae* samples, four avian postcranial elements and one *Heteropsomys* mandible) at the Oxford Radiocarbon Accelerator Unit revealed that all samples had experienced almost complete diagenetic loss of collagen, likely due to the high thermal age of Quaternary deposits in humid tropical Caribbean landscapes[19], which unfortunately prevents direct AMS ^{14}C dating of our nesophontid material. A temporal framework for interpreting body size change in *N*. *edithae* was therefore established through AMS ^{14}C dating of charcoal stratigraphically associated with the upper Nesophontes II layer, and direct uranium-series dating of nesophontid skeletal material from Nesophontes Cave and both layers at Nesophontes II Cave (Table S3).

This dual dating approach demonstrated that nearly all samples from the upper Nesophontes II layer are Holocene in age, with charcoal samples from bone-containing layers above the bone bed dating to 1,164±27 ybp (OxA26282, 4–6cm depth) and 4,113±32 ybp (OxA26283, 14–16cm depth), and four nesophontid specimens from the bone bed dating between 6,947 and 7,966 ybp. A fifth bone sample from the bone bed dated to the Late Pleistocene Bølling–Allerød interstadial, 13,486 ybp (2σ: 13,135–13,837). In contrast, all dated bone samples from the lower Nesophontes II layer and from Nesophontes Cave are

much older: two bone samples from the lower Nesophontes II layer dated to 32,682 ybp (2σ: 31,759–33,602) and 42,051 ybp (2σ: 40,789–43,307), and two bone samples from Nesophontes Cave dated to 16,382 ybp (2σ: 15,936–16,827) and 50,585 ybp (2σ: 49,074–52,089) (Table 1, Fig. 3).

Stable isotope analysis

Stable carbon isotope analysis using biogenic apatite (tooth enamel carbonate), which is widely used to assess palaeodiet in fossil mammals and is minimally susceptible to post-depositional alteration[41-43], was conducted on cheek teeth from 40 nesophontid mandibles (large morph: upper Nesophontes II layer, n=20; small morph: lower Nesophontes II layer, n=6, Nesophontes Cave, n=14). Biogenic apatite $\delta^{13}C$ values are inherited from plants at the base of local food chains, and will reflect the values for plant carbon consumed by nesophontids via their presumed invertebrate diet, with minimal trophic-level fractionation likely to occur between plant material and invertebrate prey[44]. Leaves of C_3 plants growing in forest understoreys have $\delta^{13}C$ values 2-5‰ lower than those growing in open environments[45,46], and these differences are magnified further if open areas include C_4 grasses with significantly higher $\delta^{13}C$ values, which occur today in drier parts of the insular Caribbean and are likely to have been regionally more widespread during the Late Pleistocene[47]. Although there is overlap between the $\delta^{13}C$ values shown by the two nesophontid size morphs, the two sets of values are significantly different, with lower values shown by the large morph (mean=–10.3‰ V-PDB, SD=0.98) compared to the small morph (mean=–7.9‰ V-PDB, SD=2.03) (two-tailed heteroscedastic t-test, $p<0.001$; Table S4, Fig. S2).

DISCUSSION

Our multidisciplinary investigation of a new prehistoric stratified owl deposit and neighbouring cave site overcomes many of the taphonomic problems that hinder reconstruction of Quaternary faunal change in the tropical Caribbean, and provides a temporal-ecological framework for understanding size variation in an enigmatic extinct island mammal. Our findings demonstrate that in our study sites, the smaller nesophontid size morph dates from the Last Glacial Period, whereas the larger nesophontid size morph, which was over twice its mass, instead post-dates the Last Glacial Maximum (LGM). These allochronic size morphs also show differences in $\delta^{13}C$ values that are consistent with the different distinct environmental conditions that prevailed in Puerto Rico during different periods of the late Quaternary, with the small older morph displaying an isotopic signal associated with more open savanna-type habitats typical of the Late Pleistocene, and the large younger morph displaying a signal associated with more closed forest habitats typical of the Holocene.

In contrast to spatiotemporal patterns of nesophontid diversity on both Cuba and Hispaniola, where multiple size-differentiated species co-occurred in Holocene horizons within the same landscapes[21-23], the two late Quaternary size morphs of *N*. *edithae* are not present in contemporaneous deposits within our study sites. We consider it very unlikely that multiple size morphs were coeval within this landscape during the late Quaternary but were undetected by our fossil sampling, as our abundant nesophontid measurement series are unimodal, and we also collected all other currently-recognised endemic Puerto Rican non-volant land mammals during our excavations in Nesophontes Cave and

Nesophontes II Cave[24,48]. Tytonid owl-derived mammalian prey accumulations have been demonstrated to show close ecological fidelity to landscape-level patterns of species richness and abundance in autochthonous small mammal communities[36,49], and the Nesophontes II owl deposit also contains a range of other terrestrial vertebrate taxa that vary widely in body size and ecology, including birds that range in size from small passerines and todies to large *Patagioenas* pigeons and *Saurothera* and *Crotophaga* cuckoos (Table S1). We therefore consider it highly unlikely that *Tyto cavatica* would have selectively predated only one size morph if multiple nesophontids had been contemporaneous in the local environment of the Morovis caves. Indeed, *Tyto* species that hunt across both forested and open habitats in other systems are shown to oversample small mammals in grasslands[50], suggesting that the savanna-associated small nesophontid morph should be present in the Nesophontes II owl deposit if it existed anywhere within the wider Holocene landscape across which the owl hunted. We are therefore confident that distinct size-differentiated nesophontid populations occurred in our study landscape during different periods of the late Quaternary. These results refute the original hypothesis of strong sexual dimorphism in Puerto Rican nesophontids[25], and thus raise the question of what environment factors were responsible for size variation in individuals from our study landscape.

Puerto Rican nesophontids show a marked increase in size over time, with the shift from small morph to large morph being chronologically associated with temperature increase, sea-level rise, and reduction in Puerto Rico's total land area after the LGM (Fig. 3). This shift does not align precisely with the Pleistocene–Holocene boundary; instead, the oldest dated large morph in our

study is from the Bølling–Allerød interstadial, an interval when warm, moist conditions similar to those of the Holocene also prevailed in the Caribbean region[30,31]. Interestingly, the pattern of allochronic size variation shown by Puerto Rican nesophontids across the late Quaternary does not match the predictions of either the Island Rule or Bergmann's Rule, the two main evolutionary models previously proposed to explain size change in insular small mammals[8,9,17,18]. Whereas continental small-bodied mammal lineages, including eulipotyphlans[51], typically become larger after they colonize islands (although there is considerable variation around this general trend[7]), insular vertebrate body size is positively correlated with island area and associated resource availability, which would therefore predict a decrease in nesophontid size as sea levels rose and island area shrank[52,53]. As larger body size is positively correlated with colder environments, Bergmann's Rule would also predict a decrease in nesophontid size as temperatures increased[17,18].

Instead, size change in Puerto Rican nesophontids may have been driven by an ecological shift from open savanna to closed tropical forest habitat. This shift is evidenced by the statistical difference in $\delta^{13}C$ values shown by different size morphs. Although global fluctuations in the concentration (pCO_2) and $\delta^{13}C$ value of atmospheric CO_2 are well-documented during the period covered by our samples, this variation has been measured at a maximum of ±0.3‰[54,55], which would not be enough to explain differences in $\delta^{13}C$ composition between allochronic nesophontid size morphs from the same site. Recent studies have challenged the premise of limited pCO_2 effects on plant $\delta^{13}C$ values[56] and have demonstrated that pCO_2 and $\delta^{13}C$ can exhibit strong correlations[57], making it difficult to categorically interpret the different isotopic signals shown by small

and large nesophontid size morphs as evidence of a local habitat shift, as this trend can be also affected by changes in pCO_2 beyond ±0.3‰. However, the different isotopic signals are consistent with the known regional Late Pleistocene-Holocene shift in vegetation types[29-31]. A change to tropical forest conditions in the Holocene at our study landscape is also supported by taxonomic composition of the rich avifaunal material available in the owl-deposited bone bed in the upper Nesophontes II layer, which contains several indicator species that are dependent today upon closed forest habitat (e.g. *Amazona vittata*, *Geotrygon* and *Patagioenas* pigeons, *Otus nudipes*)[58] (Table S1).

Populations of several small mammal species show larger body sizes in closed forest habitat compared to more open fragmented landscapes[59], and mammalian body sizes are higher in ecosystems with high primary productivity such as tropical rainforests[60]. However, tropical savannas can also show high primary productivity[61,62], and other studies have shown a possible trend of increasing body size across multiple small mammals in relation to increased habitat fragmentation rather than connected forest habitat, although this might reflect an 'island' isolation effect rather than being associated with changing habitat openness[63,64]. More research is required into the relationship between body size variation and habitat structure and productivity in small mammals, and into the ecosystem parameters of successive Caribbean Quaternary environments.

Direct dating of specimens demonstrates that the small nesophontid morph was present at our study landscape for over 30,000 years, from the later part of the Last Glacial Period ~50,000 ybp and across the LGM, with the youngest specimen dating from less than 16,500 ybp. The change from small morph to

large morph at this site occurred within 3,000 years, with the oldest large morph dating from ~13,500 ybp. This rapid turnover may simply reflect ecological shifts in the local distribution of two niche-differentiated nesophontid species, representing open-habitat and forest specialists that had already evolved through earlier cladogenesis and that were tracking terminal Pleistocene climate-driven changes in savanna and forest cover. Although savanna-type habitats were widely distributed across the Caribbean region during the LGM, mesic refugias are also known to have persisted on Puerto Rico through this period[31,65]. Both of these putative nesophontid species could therefore have co-occurred on the island throughout the late Quaternary but restricted to different landscapes characterized by distinct habitat types, with the savanna morph becoming replaced by the forest morph in the vicinity of the Morovis caves as open habitats were locally replaced by closed habitats. The holotype of *Nesophontes edithae* is a small morph (interpreted as a female individual by Harold E. Anthony, who described the species[25]), so if further research confirms that two nesophontid species did formerly exist on Puerto Rico, the larger-bodied species would require a new taxonomic name. Dynamic patterns of local loss and replacement are also documented in other small mammal populations in response to environmental instability and climate fluctuations during the Late Pleistocene[15,66].

It is difficult to predict the relationship between size differentiation and co-occurring community assembly in small mammal congeners[67,68], especially on islands[69,70]. However, the hypothesis of rigidly habitat-differentiated nesophontid species inhabiting exclusive landscapes with no environmental overlap contrasts with nesophontid diversity on Cuba and Hispaniola, where

multiple size-differentiated species co-occurred within the same ecosystems[21-23]. Multiple soricid eulipotyphlan species are also distributed sympatrically on several southeast Asian islands that are similar in size to Puerto Rico[71]. It is thus possible that the rapid nesophontid size shift observed at our site instead represents a punctuated evolutionary anagenetic shift within the same population. Rapid morphological and body size differentiation in response to changing environmental conditions, especially novel ecological states present on islands[72,73], has been observed in several other vertebrate populations at millennial or even multi-century scales[74-77], with smaller-bodied species able to undergo morphological change at faster rates[78]. Severe climatic change, such as that experienced by nesophontid populations at the end of the Pleistocene, is predicted to be able to prompt rapid within-population evolutionary responses in terrestrial vertebrates[79]. Interestingly, marked size increase unaccompanied by genetic differentiation is also shown by some populations of Eurasian water shrew *Neomys fodiens*[80]. Soricids also exhibit substantial phenotypically plastic seasonal changes in skull size in response to varying resource availability ('Dehnel's phenomenon')[81,82], indicating the potential for both genetic and plastic contributions to climatically-driven morphological change[79].

Our study provides an important example of mammalian body size change, identifying the likely drivers of this evolutionary shift and potentially tracing the course of an anagenetic event rather than just seeing its end-point. Size change can constitute a rapid evolutionary response to changing environmental conditions, and our findings emphasize the body size hypervariability of island mammals[72,73]. Puerto Rican nesophontids were remarkably resilient to climatic change, thus demonstrating that despite representing an evolutionarily ancient

386 'living fossil' mammal lineage[19], they retained a dynamic capacity for adaptation
387 and innovation. However, despite this evolutionary and ecological flexibility,
388 they became extinct following human introduction of invasive mammal
389 predators around 500 years ago[24,83]. Their extinction highlights the vulnerability
390 of unique island biodiversity to ongoing anthropogenic pressures[9], and acts as a
391 reminder that the historical loss of island taxa has impacted our understanding
392 of many fundamental evolutionary and ecological processes[84,85].
393
394 **LIMITATIONS OF THE STUDY**
395 The almost complete loss of organic content from all our samples unfortunately
396 prevents analysis of the evolutionary relationships between allochronic small
397 and large morphs using biomolecular phylogenetic methods (proteomics or
398 ancient DNA, which is less likely to preserve than collagen[21,86]), and previous
399 screening of samples from the upper layer failed to yield DNA[20]. We therefore
400 cannot determine whether the two morphs have a direct ancestor-descendant
401 relationship within a single anagenetic lineage or represent sister taxa that
402 evolved through older cladogenesis, and thus whether nesophontid size change
403 observed at our sites represents an ecological shift or a punctuated evolutionary
404 shift. We hope that biomolecular phylogenetic analysis is possible for better-
405 preserved specimens of both size classes, and we recommend further
406 investigation of Puerto Rican nesophontid material at sites that could have
407 sampled past savanna-forest ecotones or that occur within Holocene savanna
408 landscapes, to investigate potential co-occurrence of different size morphs or
409 persistence of the small morph into the Holocene in suitable habitats.

Due to the small size and fragmentary condition of our nesophontid samples, we were also unable to conduct uranium-series dating and stable isotope analysis upon the same specimens, meaning that we can only assign animals of known isotopic ecology to stratigraphic horizons with associated dates, rather than having direct dates for individuals that are specifically linked to open or closed habitats.

RESOURCE AVAILABILITY

Lead contact

Further information and requests for resources should be directed to and will be fulfilled by the lead contact, Samuel Turvey (samuel.turvey@ioz.ac.uk).

Materials availability

All fossil material from Nesophontes Cave and Nesophontes II Cave collected during this study is currently housed in the collections of the Institute of Zoology, Zoological Society of London (mammal and other non-bird material) and the bird collections of the Natural History Museum at Tring, Hertfordshire, UK (bird material).

Data and code availability

- All data necessary to interpret and replicate results are available in the main text and Supplemental Data, Supplemental Figures, and Supplemental Tables.
- This paper does not report original code.

Any additional information required to reanalyze the data reported in this paper is available from the lead contact upon request.

STAR METHODS

Detailed methods are provided in the online version of this paper and include the following:

- KEY RESOURCES TABLE
- METHOD DETAILS
  - Radiometric dating analyses
  - Stable isotope analysis
- QUANTIFICATION AND STATISTICAL ANALYSIS

ACKNOWLEDGEMENTS

Funding was provided by Leverhulme Early Career Fellowship ECF/2004/0410, NERC Postdoctoral Fellowship NE/D009456/1, the NERC Isotope Geoscience Facilities Steering Committee (IP/950/1106, IP/1075/1108), the Natural History Museum, and Research England. We thank Selina Brace, Liliana Dávalos, Frederick Grady, Tom Higham, Hilary Sloane, and Fundación de Investigaciones Espeleológicas del Karso Puertorriqueño.

DECLARATION OF INTERESTS

All affiliations are listed on the title page of the manuscript. All funding sources for this study are listed in the “Acknowledgements” section of the manuscript. We, the authors and our immediate family members, have no financial interests to declare. We, the authors and our immediate family members, have no

positions to declare and are not members of the journal's advisory board. We, the authors and our immediate family members, have no related patent applications or registrations to declare.

AUTHOR CONTRIBUTIONS

S.T.T. designed and oversaw the project; S.T.T., P.R. and A.V.N. collected samples; S.T.T., A.L.L., P.V.C., P.R. and J.H.C. conducted analyses; S.T.T., A.L.L. and P.V.C. wrote the paper.

REFERENCES

1. Martin, P.S., and Klein, R.G., eds. (1984). Quaternary Extinctions: A Prehistoric Revolution (University of Arizona Press).
2. Lorenzen, E.D., Nogués-Bravo, D., Orlando, L., Weinstock, J., Binladen, J., Marske, K.A., Ugan, A., Borregaard, M.K., Gilbert, M.T.P., Nielsen, R., et al. (2011). Species-specific responses of Late Quaternary megafauna to climate and humans. Nature *479*, 359–364.
3. Stuart, A.J. (2021). Vanished Giants: The Lost World of the Ice Age (University of Chicago Press).
4. Guthrie, R.D. (2003). Rapid body size decline in Alaskan Pleistocene horses before extinction. Nature *426*, 169–171.
5. Stewart, J.R. (2007). An Evolutionary Study of Some Archaeologically Significant Avian Taxa in the Quaternary of the Western Palaearctic (BAR Publishing).

6. Hill, M.E. Jr., Hill, M.G., and Wigda, C.C. (2008). Late Quaternary *Bison* diminution on the Great Plains of North America: evaluating the role of human hunting versus climate change. Quat. Sci. Rev. *27*, 1752–1771.
7. Meiri, S., Cooper, N., and Purvis, A. (2008). The island rule: made to be broken? Proc. Biol. Sci. *275*, 141–148.
8. Lomolino, M.V., van der Geer, A.A., Lyras, G.A., Palombo, M.R., Sax, D.F., and Rozzi, R. (2013). Of mice and mammoths: generality and antiquity of the island rule. J. Biogeogr. *40*, 1427–1439.
9. Rozzi, R., Lomolino, M.V., van der Geer, A.A.E., Silvestro, D., Lyons, S.K., Bover, P., Alcover, J.A., Benítez-López, A., Tsai, C.H., Fujita, M., et al. (2023). Dwarfism and gigantism drive human-mediated extinctions on islands. Science *379*, 1054–1058.
10. Lister, A.M. (1989). Rapid dwarfing of red deer on Jersey during the Last Interglacial. Nature *342*, 539–542.
11. Anderson, R.P., and Handley, C.O. (2002). Dwarfism in insular sloths: biogeography, selection, and evolutionary rate. Evolution *56*, 1045–1058.
12. Guthrie, R.D. (2004). Radiocarbon evidence of mid-Holocene mammoths stranded on an Alaskan Bering Sea island. Nature *429*, 746–749.
13. McFarlane, D.A., MacPhee, R.D.E., and Ford, D.C. (1998). Body size variability and a Sangamonian extinction model for *Amblyrhiza*, a West Indian megafaunal rodent. Quat. Res. *50*, 80–89.
14. Woods, R., Barnes, I., Brace, S., and Turvey, S.T. (2021). Ancient DNA suggests single colonisation and within-archipelago diversification of Caribbean caviomorph rodents. Mol. Biol. Evol. *38*, 84–95.

15. Brace, S., Palkopoulou, E., Dalén, L., Lister, A.M., Miller, R., Otte, M., Germonpré, M., Blockley, S.P.E., Stewart, J.R., and Barnes, I. (2012). Serial population extinctions in a small mammal indicate Late Pleistocene ecosystem instability. Proc. Natl Acad. Sci. USA *109*, 20532–20536.
16. Prost, S., Klietmann, J., van Kolfschoten, T., Guralnick, R.P., Waltari, E., Vrieling, K., Stiller, M., Nagel, D., Rabeder, G., Hofreiter, M., et al. (2013). Effects of late Quaternary climate change on Palearctic shrews. Glob. Change Biol. *19*, 1865–1874.
17. Millien, V., and Damuth, J. (2004). Climate change and size evolution in an island rodent species: new perspectives on the island rule. Evolution *58*, 1353–1360.
18. Earl of Cranbrook, and Piper, P.J. (2008). Post-Pleistocene evolution of Bornean shrews *Crocidura foetia* (Mammalia, Soricidae). Biol. J. Linn. Soc. *94*, 413–419.
19. Cooke, S.B., Dávalos, L.M., Mychajliw, A.M., Turvey, S.T., and Upham, N.S. (2017). Anthropogenic extinction dominates Holocene declines of West Indian mammals. Annu. Rev. Ecol. Evol. Syst. *48*, 301–327.
20. Brace, S., Thomas, J., Dalén, L., Burger, J., MacPhee, R.D.E., Barnes, I., and Turvey, S.T. (2017). Evolutionary history of the Nesophontidae, the last unplaced Recent mammal family. Mol. Biol. Evol. *33*, 3095–3103.
21. Buckley, M., Harvey, V.L., Orihuela, J., Mychajliw, A.M., Keating, J.N., Almonte Milan, J.N., Lawless, C., Chamberlain, A.T., Egerton, V.M., and Manning, P.L. (2020). Collagen sequence analysis reveals evolutionary history of extinct West Indies *Nesophontes* (island-shrews). Mol. Biol. Evol. *37*, 2931–2943.

22. Woods, R., Turvey, S.T., Brace, S., McCabe, C.V., Dalén, L., Rayfield, E.J., Brown, M.J.F., and Barnes, I. (2020). Rapid size change associated with intra-island evolutionary radiation in extinct Caribbean "island-shrews". BMC Evol. Biol. *20*, 106.

23. Orihuela León, J. (2023). Revision of the extinct island-shrews *Nesophontes* (Mammalia: Eulipotyphla: Nesophontidae) from Cuba. J. South Am. Earth Sci. *130*, 104544.

24. Turvey, S.T., Oliver, J.R., Narganes Storde, Y., and Rye, P. (2007). Late Holocene extinction of Puerto Rican native land mammals. Biol. Lett. *3*, 193–196.

25. Anthony, H.E. (1916). Preliminary diagnosis of an apparently new family of insectivores. Bull. Am. Mus. Nat. Hist. *35*, 725–728.

26. Morgan, G.S., MacPhee, R.D.E., Woods, R., and Turvey, S.T. (2019). Late Quaternary fossil mammals from the Cayman Islands, West Indies. Bull. Am. Mus. Nat. Hist. *428*, 1–79.

27. Choate, J.R., and Birney, E.C. (1968). Sub-recent Insectivora and Chiroptera from Puerto Rico, with the description of a new bat of the genus *Stenoderma*. J. Mamm. *49*, 400–412.

28. McFarlane, D.A. (1999). A note on dimorphism in *Nesophontes edithae* (Mammalia: Insectivora), an extinct island-shrew from Puerto Rico. Carib. J. Sci. *35*, 142–143.

29. Pregill, G.K., and Olson, S.L. (1981). Zoogeography of West Indian vertebrates in relation to Pleistocene climatic cycles. Annu. Rev. Ecol. Syst. *12*, 75–98.

30. Hodell, D.A., Anselmetti, F.S., Ariztegui, D., Brenner, M., Curtis, J.H., Gilli, A., Grzesik, D.A., Guilderson, T.J., Müller, A.D., Bush, M.B., et al. (2008). An 85-ka

record of climate change in lowland Central America. Quat. Sci. Rev. *27*, 1152–1165.

31. Harrison, E.J., Willenbring, J.K., and Brocard, G.Y. (2021). Quaternary record of terrestrial environmental change in response to climatic forcing and anthropogenic perturbations, in Puerto Rico. Quat. Sci. Rev. *253*, 106770.
32. Hastings, A.K., Krigbaum, J., Steadman, D.W., and Albury, N.A. (2014). Domination by reptiles in a terrestrial food web of the Bahamas prior to human occupation. J. Herpetol. *48*, 380–388.
33. Cooke, S.B., and Crowley, B.E. (2018). Deciphering the isotopic niches of now-extinct Hispaniolan rodents. J. Vertebr. Paleontol. *38*, e1510414.
34. LeFebvre, M.J., deFrance, S.D., Kamenov, G.D., Keegan, W.F., and Krigbaum, J. (2019). The zooarchaeology and isotopic ecology of the Bahamian hutia (*Geocapromys ingrahami*): evidence for pre-Columbian anthropogenic management. PLoS ONE *14*, e0220284.
35. Pregill, G.K. (1981). Late Pleistocene herpetofaunas from Puerto Rico. Univ. Kansas Mus. Nat. Hist. Misc. Publ. *71*, 1–72.
36. Andrews, P. (1990). Owls, Caves and Fossils (Natural History Museum Publications).
37. Wetmore, A. (1920). Five new species of birds from cave deposits in Porto Rico. Proc. Biol. Soc. Washington *33*, 77–82.
38. Bloch, J.I., Rose, K.D., and Gingerich, P.D. (1998). New species of *Batodonoides* (Lipotyphla, Geolabididae) from the early Eocene of Wyoming: smallest known mammal? J. Mammal. *79*, 804–827.

578 39. Worthy, T.H., and Holdaway, R.N. (1996). Taphonomy of two Holocene
579 microvertebrate deposits, Takaka Hill, Nelson, New Zealand, and
580 identification of the avian predator responsible. Hist. Biol. *12*, 1–24.
581 40. Burnham, K.K., Burnham, W.I., and Newton, I. (2009). Gyrfalcon *Falco*
582 *rusticolus* post-glacial colonization and extreme long-term use of nest-sites
583 in Greenland. Ibis *151*, 514–522.
584 41. Lee-Thorp, J.A., Sealy, J.C., and van der Merwe, N.J. (1989). Stable carbon
585 isotope ratio differences between bone collagen and bone apatite, and their
586 relationship to diet. J. Archaeol. Sci. *16*, 585–599.
587 42. Botha, J., Lee-Thorp, J., and Chinsamy, A. (2005). The palaeoecology of the
588 non-mammalian cynodonts *Diademodon* and *Cynognathus* from the Karoo
589 Basin of South Africa, using stable light isotope analysis. Palaeogeogr.
590 Palaeoclimatol. Palaeoecol. *223*, 303–316.
591 43. Sponheimer, M., Codron, D., Passey, B.H., de Ruiter, D.J., Cerling, T.E., and Lee-
592 Thorp, J.A. (2009). Using carbon isotopes to track dietary change in modern,
593 historical, and ancient primates. Am. J. Phys. Anthropol. *140*, 661–670.
594 44. DeNiro, M.J., and Epstein, S. (1978). Influence of diet on the distribution of
595 carbon isotopes in animals. Geochim. Cosmochim. Acta *42*, 495–506.
596 45. Tieszen, L.L., and Boutton, T.W. (1989). Stable carbon isotopes in terrestrial
597 ecosystem research. In Stable Isotopes in Ecological Research, P.W. Rundel,
598 J.R. Ehleringer, and K.A. Nagy, eds. (SpringerVerlag), pp. 167–195.
599 46. Heaton T.H.E. (1999). Spatial, species and temporal variations in the $^{13}C/^{12}C$
600 ratios of C3 plants: implications for palaeodiet studies. J. Archaeol. Sci. *26*,
601 637–649.

602 47. Lane, C.S., Horn, S.P., Mora, C.I., Orvis, K.H., and Finkelstein, D.B. (2011).
603 Sedimentary stable carbon isotope evidence of late Quaternary vegetation
604 and climate change in highland Costa Rica. *J. Paleolimnol. 45*, 323–338.
605 48. Bover, P., and MacPhee, R.D.E. (2007). Variability in the femur of
606 *Elasmodontomys obliquus* and its bearing on the status of *Tainotherium valei.*
607 Simposio Internacional de Zoología *7*, 119–120.
608 49. Terry, R.C. (2010). On raptors and rodents: testing the ecological fidelity and
609 spatiotemporal resolution of cave death assemblages. Paleobiol. *36*, 137–
610 160.
611 50. Torre, I., Arrizabalaga, A., and Flaquer, C. (2004). Three methods for
612 assessing richness and composition of small mammal communities. J.
613 Mammal. *85*, 524–530.
614 51. Moncunill-Solé, B., Jordana, X., and Köhler, M. (2016). How common is
615 gigantism in insular fossil shrews? Examining the 'Island Rule' in soricids
616 (Mammalia: Soricomorpha) from Mediterranean Islands using new body
617 mass estimation models. Zool. J. Linn. Soc. *178*, 163–182.
618 52. Burness, G.P., Diamond, J., and Flannery, T. (2001). Dinosaurs, dragons, and
619 dwarfs: the evolution of maximal body size. Proc. Natl Acad. Sci. USA *98*,
620 14518–14523.
621 53. van der Geer, A.A.E., van den Bergh, G.D., Lyras, G.A., Prasetyo, U.W., Awe
622 Due, R., Setiyabudi, E., and Drinia, H. (2016). The effect of area and isolation
623 on insular dwarf proboscideans. J. Biogeogr. *43*, 1656–1666.
624 54. Leuenberger, M., Siegenthaler, U., and Langway, C.C. (1992). Carbon isotope
625 composition of atmospheric CO_2 during the last ice age from an Antarctic ice
626 core. Nature *357*, 488–490.

627 55. Trudinger, C.M., Enting, I.G., Francey, R.J., Etheridge, D.M., and Rayner, P.J.
628 (1999). Long-term variability in the global carbon cycle inferred from a high-
629 precision CO_2 and δ13C ice-core record. Tellus B *51*, 233–248.
630 56. Hare, V.J., Loftus, E., Jeffrey, A., and Bronk Ramsey, C. (2018). Atmospheric
631 CO_2 effect on stable carbon isotope composition of terrestrial fossil archives.
632 Nat. Commun. *9*, 252.
633 57. Bump, J.K., Fox-Dobbs, K., Bada, J.L., Koch, P.L., Peterson, R.O., and Vucetich,
634 J.A. (2007). Stable isotopes, ecological integration and environmental
635 change: wolves record atmospheric carbon isotope trend better than tree
636 rings. Proc. Biol. Sci. *274*, 2471–2480.
637 58. Raffaele, H.A. (1989). A Guide to the Birds of Puerto Rico and the Virgin
638 Islands (Princeton University Press).
639 59. Lomolino, M.V., and Perault, D.R. (2007). Body size variation of mammals in a
640 fragmented, temperate rainforest. Conserv. Biol. *21*, 1059–1069.
641 60. Aava, B. (2001). Primary productivity can affect mammalian body size
642 frequency distributions. Oikos *93*, 205–212.
643 61. Grace, G., San José, J., Meir, P., Miranda, H.S., and Montes, R.A. (2006).
644 Productivity and carbon fluxes of tropical savannas. J. Biogeogr. *33*, 387–400.
645 62. Murphy, B.P., and Bowman, D.M.J.S. (2012). What controls the distribution of
646 tropical forest and savanna? Ecol. Lett. *15*, 748–758.
647 63. Schmidt, N.M., and Jensen, P.M. (2003). Changes in mammalian body length
648 over 175 years—adaptations to a fragmented landscape? Conserv. Ecol. *7(2)*,
649 6.

650 64. Fietz, J., and Weis-Dootz, T. (2012). Stranded on an island: consequences of
651 forest fragmentation for body size variations in an arboreal mammal, the
652 edible dormouse (*Glis glis*). Popul. Ecol. *54*, 313–320.
653 65. Barker, B.S., Rodríguez-Robles, J.A., and Cook, J.A. (2015). Climate as a driver
654 of tropical insular diversity: comparative phylogeography of two ecologically
655 distinctive frogs in Puerto Rico. Ecography *38*, 769–781.
656 66. Palkopoulou, E., Baca, M., Abramson, N.I., Sablin, M., Socha, P., Nadachowski,
657 A., Prost, S., Germonpré, M., Kosintsev, P., Smirnov, N.G., et al. (2016).
658 Synchronous genetic turnovers across Western Eurasia in Late Pleistocene
659 collared lemmings. Glob. Change Biol. *22*, 1710–1721.
660 67. Simberloff, D., and Boecklen, W. (1981). Santa Rosalia reconsidered: size
661 ratios and competition. Evolution *35*, 1206–1228.
662 68. Eadie, J.M., Broekhoven, L., and Colgan, P. (1987). Size ratios and artifacts:
663 Hutchinson's Rule revisited. Am. Nat. *129*, 1–17.
664 69. Okie, J.G., and Brown, J.H. (2009). Niches, body sizes, and the disassembly of
665 mammal communities on the Sunda Shelf islands. Proc. Natl Acad. Sci. USA
666 *106 (suppl. 2)*, 19679–19684.
667 70. O'Connell, M.A., and Hallett, J.G. (2019). Community ecology of mammals:
668 deserts, islands, and anthropogenic impacts. J. Mammal. *100*, 1019–1043.
669 71. Esselstyn, J.A., Maher, S.P., and Brown, R.M. (2011). Species interactions
670 during diversification and community assembly in an island radiation of
671 shrews. PLoS ONE *6*, e21885.
672 72. Millien, V. (2006). Morphological evolution is accelerated among island
673 mammals. PLoS Biol. *4*, e321.

73. Millien, V. (2011). Mammals evolve faster on smaller islands. Evolution *65*, 1935–1944.

74. Hofman, C.A., Rick, T.C., Hawkins, M.T.R., Funk, W.C., Ralls, K., Boser, C.L., Collins, P.W., Coonan, T., King, J.L., Morrison, S.A., et al. (2015). Mitochondrial genomes suggest rapid evolution of dwarf California Channel Islands foxes (*Urocyon littoralis*). PLoS ONE *10*, e0118240.

75. Rozzi, R., and Lomolino, M.V. (2017). Rapid dwarfing of an insular mammal—the feral cattle of Amsterdam Island. Sci. Rep. *7*, 8820.

76. Kouvari, M., Herrel, A., and Cornette, R. (2021). Humans and climate as possible drivers of the morphology and function of the mandible of *Suncus etruscus* in Corsica. J. Archaeol. Sci. *132*, 105434.

77. Andrea, C. (2022). As fast as a hare: did intraspecific morphological change bring the Hallands Väderö Island population of *Lepus timidus* close to interspecific differences in less than 150 years? Zoology *152*, 126014.

78. Zimova, M., Weeks, B.C., Willard, D.E., and Winger, B.M. (2023). Body size predicts the rate of contemporary morphological change in birds. Proc. Natl Acad. Sci. USA *120*, e2206971120.

79. Catullo, R.A., Llewelyn, J., Phillips, B.L., and Moritz, C.C. (2019). The potential for rapid evolution under anthropogenic climate change. Curr. Biol. *29*, R996–R1007.

80. Balmori-de la Puente, A., Nores, C., Román, J., Fernández-González, A., Aymerich, P., Gosálbez, J., Escoda, L., and Castresana, J. (2019). Size increase without genetic divergence in the Eurasian water shrew *Neomys fodiens*. Sci. Rep. *9*, 17375.

698 81. Lázaro, J. & Dechmann, D.K.N. (2021). Dehnel's phenomenon. Curr. Biol. *31*,
699 R459–R466.
700 82. Taylor, J.R.E., Muturi, M., Lázaro, J., Zub, K., and Dechmann, D.K.N. (2022).
701 Fifty years of data show the effects of climate on overall skull size and the
702 extent of seasonal reversible skull size changes (Dehnel's phenomenon) in
703 the common shrew. Ecol. Evol. *12*, e9447.
704 83. MacPhee, R.D.E., Flemming, C., and Lunde, D.P. (1999). "Last occurrence" of
705 the Antillean insectivoran *Nesophontes*: radiometric dates and their
706 interpretation. Am. Mus. Novit. *3261*, 1–20.
707 84. Boyer, A.G., and Jetz, W. (2014). Extinctions and the loss of ecological
708 function in island bird communities. Glob. Ecol. Biogeogr. *23*, 679–688.
709 85. Faurby, S., and Svenning, J.C. (2015). Historic and prehistoric human-driven
710 extinctions have reshaped global mammal diversity patterns. Divers. Distrib.
711 *21*, 1155–1166.
712 86. Nakamura, Y., Waku, D., Wakiyama, Y., Watanabe, Y., Koganebuchi, K.,
713 Nagaoka, T., Hirata, K., Ohashi, J., Takahashi, R., Yoneda, M., et al. (2024).
714 Collagen of ancient bones gives an indication of endogenous DNA
715 preservation based on next-generation sequencing technology. Anthropol.
716 Sci. *132*, 143–150.
717 87. Svensson, A., Andersen, K.K., Bigler, M., Clausen, H.B., Dahl-Jensen, D., Davies,
718 S.M., Johnsen, S.J., Muscheler, R., Parrenin, F., Rasmussen, S.O., et al. (2008). A
719 60 000 year Greenland stratigraphic ice core chronology. Clim. Past *4*, 47–57.
720 88. van Calsteren, P., and Thomas, L.E. (2012). Quantitation of protactinium,
721 ^{231}Pa in abyssal carbonate. J. Anal. At. Spectrom. *27*, 952–956.

722 89. Edwards, R.L., Chen, J.H., and Wasserburg, G.J. (1987). ^{238}U–^{234}U–^{230}Th–^{232}Th
723 systematics and the precise measurement of time over the past 500,000
724 years. Earth Planet. Sci. Lett. *81*, 175–192.
725 90. Turner, S., Hawkesworth, C., van Calsteren, P., Heath, E., Macdonald, R., and
726 Black, S. (1996). U-series isotopes and destructive plate margin magma
727 genesis in the Lesser Antilles. Earth Planet. Sci. Lett. *142*, 191–207.
728 91. van Calsteren, P., and Thomas, L. (2006). Uranium-series dating applications
729 in natural environmental science. Earth-Sci. Rev. *75*, 155–175.
730 92. Pike, A.W.G., Hedges, R.E.M., and van Calsteren, P. (2001). U-series dating of
731 bone using the diffusion-adsorption model. Geochim. Cosmochim. Acta *66*,
732 4273–4286.

733 **Table 1.** AMS ^{14}C dates on charcoal and uranium-series dates on *Nesophontes*

734 bones from the Morovis caves, Puerto Rico (N Cave = Nesophontes Cave, N-II

735 Cave = Nesophontes II Cave).

736

Horizon	**Specimen**	**Method**	**Lab number**	**Date, BP (2σ range)**	**Detrital-corrected date, BP (2σ range)**	**$\delta^{13}C$**
N-II Cave, upper layer (4–6cm)	charcoal	AMS ^{14}C	OxA26282	1164 (1137–1191)	—	-26.48
N-II Cave, upper layer (14–16cm)	charcoal	AMS ^{14}C	OxA26283	4113 (4081–4145)	—	-26.28
N-II Cave, upper layer (20–24 cm)	mandible	U-series	—	7060 (6913–7207)	6947 (6743–7151)	—
N-II Cave, upper layer (20–24 cm)	mandible	U-series	—	7669 (7532–7806)	7640 (7448–7832)	—
N-II Cave, upper layer (20–24 cm)	mandible	U-series	—	7749 (7601–7897)	7657 (7450–7864)	—
N-II Cave, upper layer (20–24 cm)	mandible	U-series	—	7982 (7828–8136)	7966 (7748–8184)	—
N-II Cave, upper layer (20–24 cm)	maxilla	U-series	—	13,500 (13,251–13,749)	13,486 (13,135–13,837)	—
N-II Cave, lower layer	mandible	U-series	—	32,698 (32,046–33,349)	32,682 (31,759–33,602)	—
N-II Cave, lower layer	mandible	U-series	—	42,057 (41,165–42,946)	42,051 (40,789–43,307)	—
N Cave	mandible	U-series	—	16,393 (16,078–16,708)	16,382 (15,936–16,827)	—
N Cave	mandible	U-series	—	50,783 (49,711–51,851)	50,585 (49,074–52,089)	—

737

738 **Figures**

739

740 **Fig. 1.** Puerto Rican late Quaternary fossil sites where nesophontid material was
741 collected. **A**, Location of Morovis caves in Puerto Rico. **B**, Interior of Nesophontes
742 II Cave. **C**, Entrance to Nesophontes II Cave (indicated with arrow). Photograph
743 taken from southern entrance of Nesophontes Cave, with slope deposit at cave
744 entrance shown to the right, demonstrating the immediate proximity of the two
745 caves. **D**, Plan view of Nesophontes II Cave. **E**, Excavated section at Nesophontes
746 II Cave, showing dense bone layer at 20–24 cm depth and stratigraphic
747 distribution of large and small nesophontid size morphs. Scale bar represents 15
748 cm.

749

750 **Fig. 2.** Nesophontid size morphs from the Morovis caves, Puerto Rico. **A-C**, Large
751 morph from upper layer at Nesophontes II Cave, showing varying intactness of
752 specimens from the owl deposit. Top image reversed for comparison with other
753 specimens. **D**, Small morph from Nesophontes Cave, showing partial veneer with
754 thin calcite coating indicative of older deposition. Scale bar = 5 mm.

755

756 **Fig. 3.** Dated temporal distribution of small and large nesophontid size morphs
757 at the Morovis caves across late Quaternary climatic fluctuations (illustrated by
758 NGRIP $\delta^{18}O$ curve)[87] until extinction in the late Holocene.

STAR Methods

KEY RESOURCES TABLE

REAGENT or RESOURCE	SOURCE	IDENTIFIER
Deposited data		
Morphometric data for nesophontid material from Nesophontes Cave and Nesophontes II Cave, analysed data	This paper	Table S2, Fig. S1
AMS ^{14}C data for charcoal from Nesophontes II Cave, raw data	This paper	Table 1
Uranium-series data for nesophontid material from Nesophontes Cave and Nesophontes II Cave, raw data	This paper	Table 1, Table S3, Fig. S2
Stable isotope data (carbon and oxygen) for nesophontid material from Nesophontes Cave and Nesophontes II Cave, raw data	This paper	Table S4
Bird fossils from Nesophontes II Cave, raw data	This paper	Table S1
Software and algorithms		
R v.4.2.2	R Foundation for Statistical Computing, Vienna, Austria	https://cran.r-project.org/

METHOD DETAILS

Radiometric dating analyses

Radiocarbon dating of specimens by accelerator mass spectrometry (AMS) was carried out at the University of Oxford, UK.

Uranium-series analyses were carried out at the NERC-Open University Uranium-Series Facility laboratories at the Open University, Milton Keynes, UK, following standard methods[88]. Bone samples selected for U-series analysis (<0.5g) were extracted from the internal surface of specimens using a hand-held Dremel drill, rinsed in iso-propyl alcohol and dilute nitric acid, and completely dissolved in double-distilled concentrated nitric acid. A mixed ^{229}Th/^{236}U spike was added, which was calibrated against gravimetric standards prepared from

776 CRM112a for uranium and CRM3159 for thorium. Uranium and thorium
777 fractions were separated on 2-mL anion exchange columns[89], and were both
778 diluted to 10 ppb and run on the Nu Instruments Multi-Collector Inductively
779 Coupled Plasma Mass Spectrometer (MC-ICP-MS)[90]. A dynamic peak-switching
780 routine was employed measuring $^{234}U/^{236}U$ and $^{235}U/^{236}U$ (a proxy for ^{238}U,
781 assuming a natural $^{238}U/^{235}U$ ratio of 137.88) and separately for $^{230}Th/^{229}Th$ and
782 $^{232}Th/^{229}Th$ (^{232}Th abundance is not required for age calculation but was
783 measured to monitor detrital Th input)[91]. A standard sample bracketing
784 technique was used for the Nu plasma to monitor and correct for drift. Two
785 internal solution standards and one rock standard were used to assess external
786 reproducibility. Two total procedure blanks for ^{238}U and ^{232}Th (run in parallel
787 with these samples) yielded 9 pg and 13 pg, respectively, which are insignificant
788 for the measured samples. Ages and fully propagated uncertainties were
789 calculated using standard methods[88,92]. Detrital corrections to account for the
790 fraction of ^{230}Th that is not authigenic were made on the assumption that the
791 detritus has Th/U=3.12 and is in secular equilibrium; the magnitude of the
792 correction is small, and corrected ages are within the 2σ uncertainty range of
793 uncorrected ages.
794
795 **Stable isotope analysis**
796 Analysis was conducted at the National Environmental Isotope Facility, British
797 Geological Survey, Keyworth, UK. Teeth were cleaned by ultrasonication in
798 distilled water, rinsing three times. Roots were removed; samples were too small
799 to separate dentine from enamel, but given the lack of collagen preservation in
800 the samples (see above), any remaining organic material will have been removed

with the subsequent NaOCl wash. Samples <10mg in weight were either combined with other teeth from the same mandible (to achieve a minimum of 10mg weight) or analyzed whole after the 2% NaOCl stage. Clean, trimmed teeth were crushed to a powder, placed in 2% NaOCl overnight to remove organic matter, and washed five times by centrifugation. The powder was then placed in 0.1M acetic acid for two hours and washed five times by centrifugation to remove any carbonate adsorbed onto the apatite crystal surface. Average loss of sample during preparation was 20%. Approximately 1-1.5mg of the resulting structural carbonate was loaded into glass vials and transferred to a GVMultiprep system for CO_2 conversion using anhydrous phosphoric acid at 90°C. The resultant CO_2 was cleaned and collected cryogenically for isotope analysis using a GV IsoPrime dual inlet mass spectrometer. Isotope values ($\delta^{13}C$) are reported as per mille (‰) deviations of isotopic ratios ($^{13}C/^{12}C$) calibrated to the V-PDB scale using a within-run laboratory standard (Keyworth Carrara Marble, KCM) that is scaled against NBS standards (NBS-18 and NBS-19). The analytical precision of CO_2, assessed by multiple analyses of KCM, is <0.02‰ for $\delta^{13}C$ (1σ, n=14). The analytical precision for multiple analyses of an archaeological enamel standard was <0.03‰ for $\delta^{13}C$ (1σ, n=6).

QUANTIFICATION AND STATISTICAL ANALYSIS

All statistical analyses were carried out using R v.4.2.2 https://cran.r-project.org/. Statistical tests included:

1) **One-tailed heteroscedastic t-tests** to test whether *Nesophontes* specimens from the upper layer of Nesophontes II Cave are significantly larger than specimens from Nesophontes Cave. These t-tests included comparisons of eight

826 mandibular characters (comparative sample sizes: upper Nesophontes II layer,
827 n=19-99; Nesophontes Cave, n=10-21) and eight femoral characters
828 (comparative sample sizes: upper Nesophontes II layer, n=8-113; Nesophontes
829 Cave, n=10-26). Full details of data and test statistics for comparisons of all 16
830 characters are reported in Table S2 and are summarized in the "Morphometric
831 comparisons" section of the main Results.
832 2) **Two-tailed heteroscedastic t-test** to test whether the $\delta^{13}C$ values shown by
833 the two nesophontid size morphs are significantly different. This t-test included
834 comparison of n=20 large morph specimens (mean=−10.3‰ V-PDB, SD=0.98)
835 and n=20 small morph specimens (mean=−7.9‰ V-PDB, SD=2.03). The data
836 used for this statistical comparison are reported in Table S4 and Figure S2, and
837 the data summary and test statistic are reported in the "Stable isotope analysis"
838 section of the main Results.
839
840 **Table S1.** Bird material from Nesophontes II Cave.

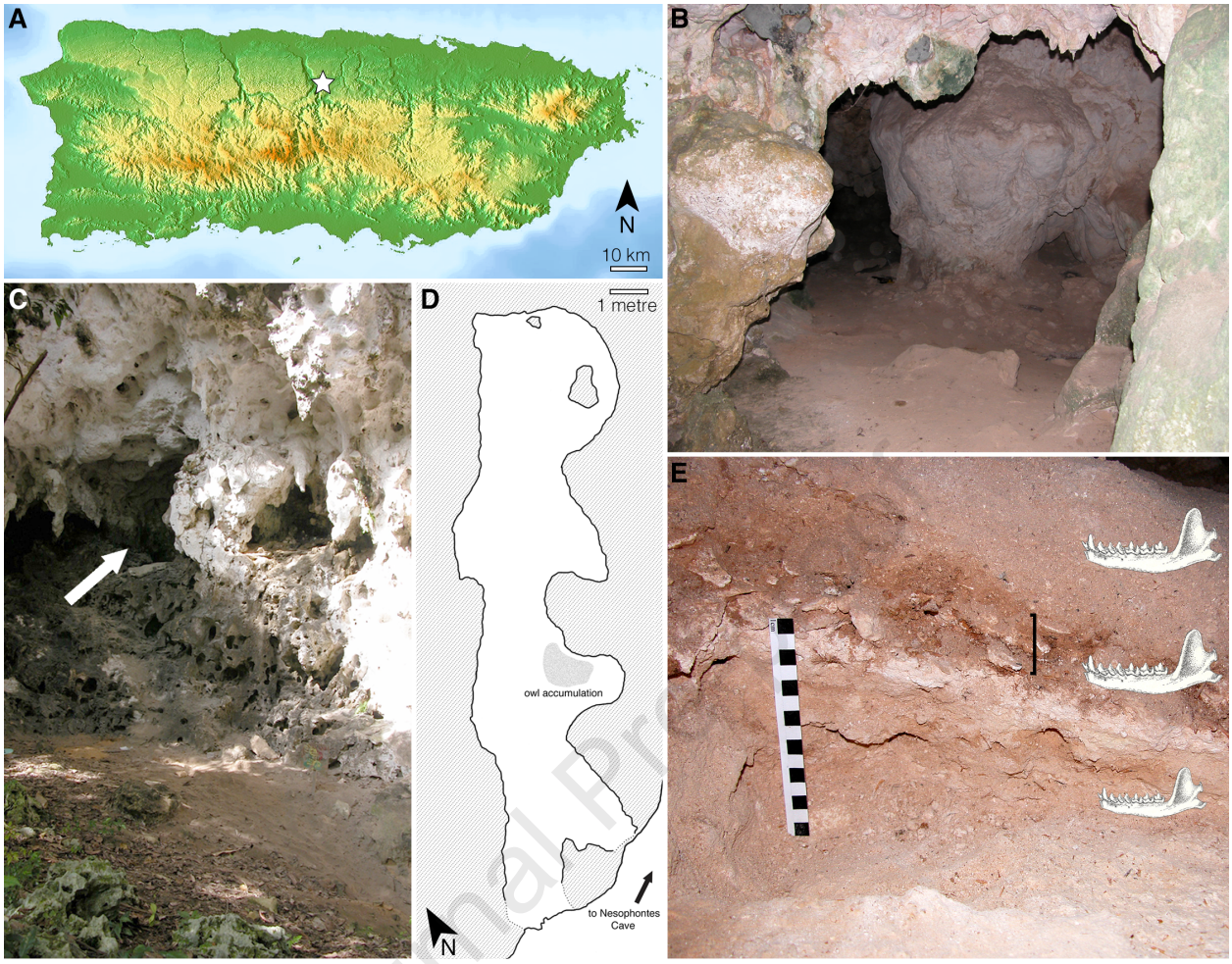

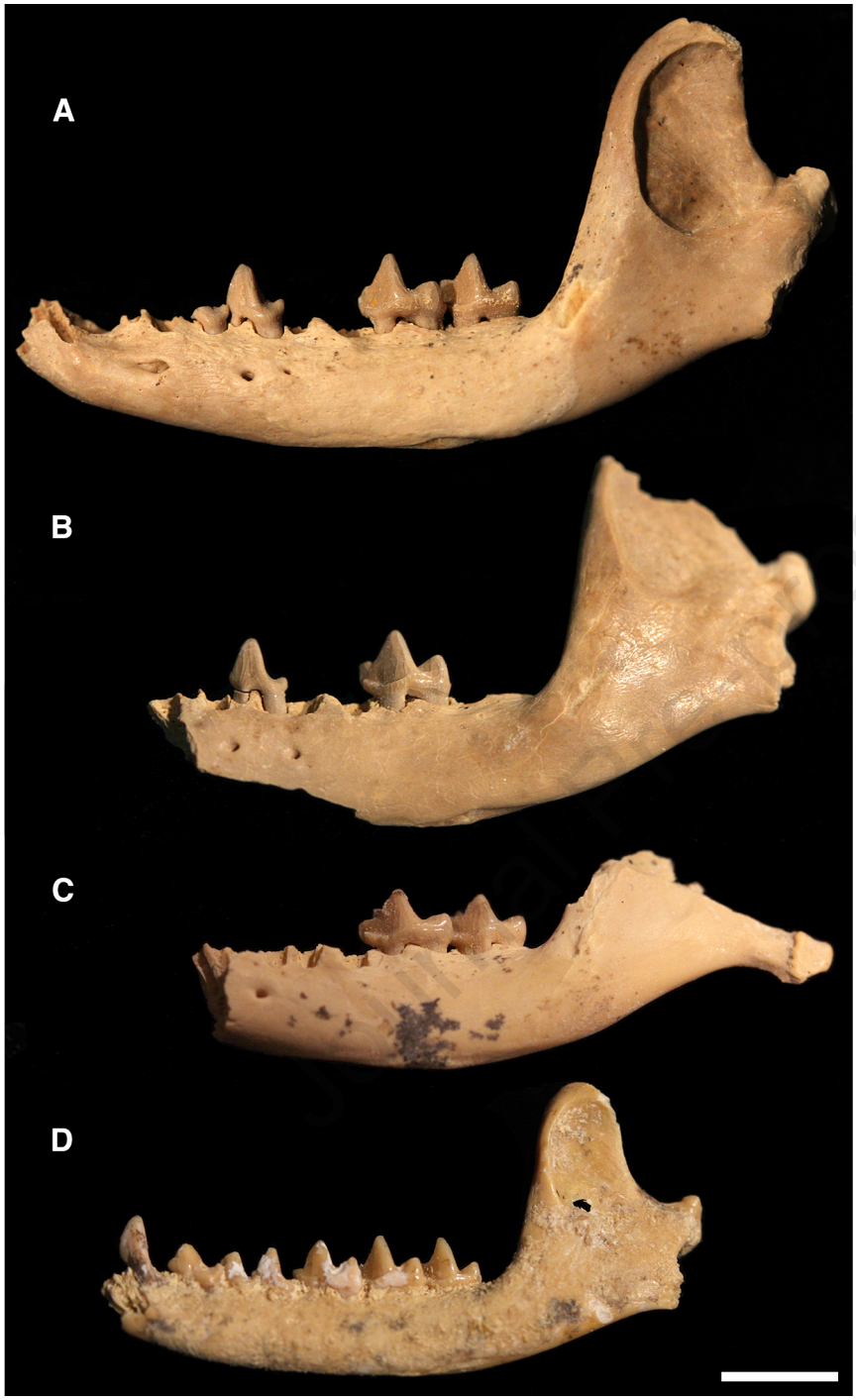

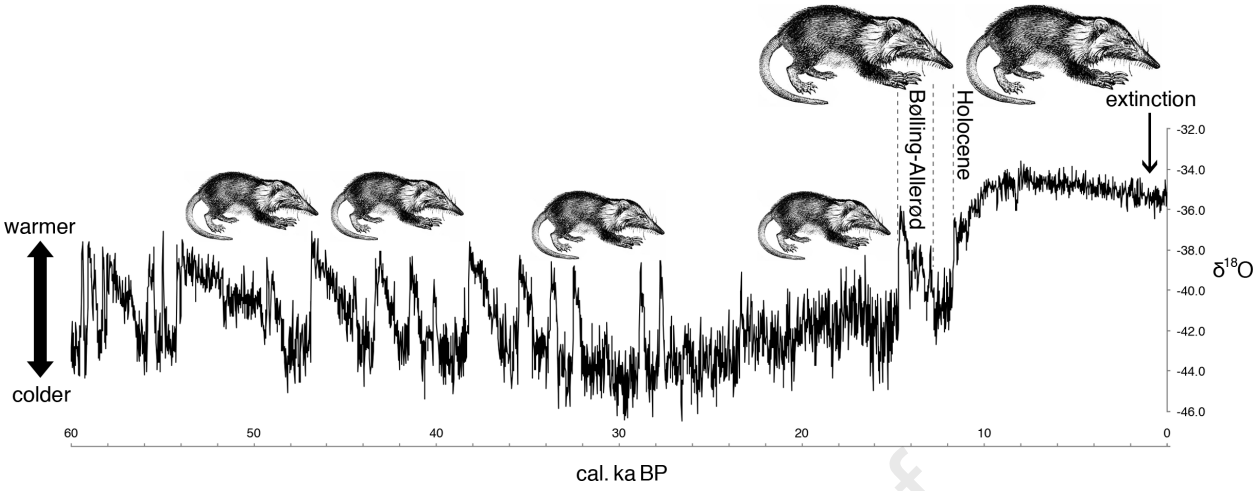

- The extinct Caribbean island-shrew *Nesophontes edithae* showed major size variation
- A small morph occurred in the LGM and was replaced by a large morph in the Holocene
- Isotopic data show size change was linked to a shift from savanna to forest habitat
- Size change may represent a rapid evolutionary response to severe climatic change

KEY RESOURCES TABLE

REAGENT or RESOURCE	SOURCE	IDENTIFIER
Deposited data		
Morphometric data for nesophontid material from Nesophontes Cave and Nesophontes II Cave, analysed data	This paper	Table S2, Fig. S1
AMS ^{14}C data for charcoal from Nesophontes II Cave, raw data	This paper	Table 1
Uranium-series data for nesophontid material from Nesophontes Cave and Nesophontes II Cave, raw data	This paper	Table 1, Table S3, Fig. S2
Stable isotope data (carbon and oxygen) for nesophontid material from Nesophontes Cave and Nesophontes II Cave, raw data	This paper	Table S4
Bird fossils from Nesophontes II Cave, raw data	This paper	Table S1
Software and algorithms		
R v.4.2.2	R Foundation for Statistical Computing, Vienna, Austria	https://cran.r-project.org/